Engineering Geology 161 (2013) 26–33

Contents lists available at SciVerse ScienceDirect

Engineering Geology

journal homepage: www.elsevier.com/locate/enggeo

Microtremors' HVSR and its correlation with surface geology and damage observed after the 2010 Maule earthquake (Mw 8.8) at Talca and Curicó, Central Chile

F. Leyton [a,*], S. Ruiz [b], S.A. Sepúlveda [c], J.P. Contreras [d], S. Rebolledo [c], M. Astroza [e]

[a] Dept. Civil Engineering, Universidad Diego Portales, Santiago, Chile
[b] Dept. Geophysics, Universidad de Chile, Santiago, Chile
[c] Dept. Geology, Universidad de Chile, Santiago, Chile
[d] Servicio Nacional de Geología y Minería, Santiago, Chile
[e] Dept. Civil Engineering, Universidad de Chile, Santiago, Chile

ARTICLE INFO

Article history:
Received 23 June 2012
Received in revised form 7 March 2013
Accepted 14 April 2013
Available online 28 April 2013

Keywords:
Microtremors
Resonance frequency
Surface geology
Macroseismic intensities

ABSTRACT

Nowadays, microtremors' horizontal-to-vertical spectral ratio (HVSR) has been extensively used in the estimation of the predominant vibration frequency of soils, mainly for microzonation purposes. In the present study, we show results from extensive microtremor measurements performed at the cities of Talca and Curicó, Central Chile. We found a strong correlation between surface geology and microtremors' HVSR, even in complex geological settings. Considering the damage produced by the 2010 Maule earthquake (Mw 8.8), we also estimated high-density macroseismic intensities at these cities, with values ranging from VI up to VIII on the MSK64 scale. We believe that the main responsible of these variations are the surface geological conditions, also reflected in the variations of the resonance frequencies of the soils. The evidence presented here supports the use of microtremors' HVSR in combination with surface geology to improve seismic microzonation studies, particularly in an Andean context.

1. Introduction

The amplification produced by site conditions plays a key role in establishing the damaging potential of incoming seismic waves from major earthquakes (e.g. Borcherdt, 1970). Since the early observations made by Milne (1898) showing clear amplifications that sedimentary deposits produce on seismic ground motions, several studies have been devoted to this topic. For example, most of the damage produced by the 1989 Loma Prieta earthquake was directly related to the site response (Holzer, 1994), as well as the effects of the 1994 Northridge earthquake, producing pockets of heavy damage within 1 km from regions with largely undamaged zones in Los Angeles (Wald and Mori, 2000). The pattern of damage in Mexico City produced by the 1985 Michoacan earthquake showed that the effect of local site conditions was very important (Singh et al., 1988), suggesting a strong amplification difference between rock and paleolake-bed sites (Ordaz and Singh, 1992). Nevertheless, we found a lack of studies analyzing the damage produced by large interplate subduction earthquakes (Mw > 8.0), especially in an Andean context. Hence, the importance of methodologically analyzing the effects of the recent 2010 Maule earthquake (Mw 8.8) and its relation with surface conditions.

The cities of Talca and Curicó, Central Chile, are located in an area where large earthquakes frequently occur (see Figure 1). Despite the fact that these are not located near the sources of large historical earthquakes, typically interplate subduction earthquakes with coastal or off-shore epicenters (as those shown in Figure 1), these hinterland cities systematically have shown higher seismic intensities than neighboring localities. From the early observations of Montessus de Ballore after the 1906 Valparaíso earthquake (Mw 8.2), Curicó presented an intensity that, on the 10 degree 1902 Mercalli scale (IM-02), was equal to IM-02 = IX; while neighboring cities presented lower values: Teno (IM-02 = VI) and Rauco (IM-02 = VI) (Montessus de Ballore, 1915). At Talca, the damage levels were lower (IM-02 = VIII); nevertheless, this value was larger than nearby localities, such as Pelarco (IM-02 = VII–VIII) and Pencahue (almost no damage was reported). On the other hand, for the 1928 Talca earthquake (Mw 7.7), this city was strongly damaged, reaching a Modified Mercalli Intensity IMM = VIII–IX, while nearby cities did not exceed intensity VIII (Astroza et al., 2002). Note that, at that time, Talca was mostly located over volcanic ash deposits, shown in Fig. 2a. For the 1985 Valparaíso earthquake (Mw 8.0), the damage produced was lower due to the large epicentral distance of both cities. Nevertheless, Barrientos and Cancino (1991) showed that MSK64 seismic intensity was larger on the Northern part of Talca (IMSK64 = VII–VIII), located over the volcanic ash deposits, compared to the Southwestern part (IMSK64 = VII), located over fluvial and alluvial deposits. For nearby

* Corresponding author. Tel.: +56 2676 2444; fax: +56 2676 2402.
E-mail address: felipe.leyton@udp.cl (F. Leyton).

0013-7952/$ – see front matter
http://dx.doi.org/10.1016/j.enggeo.2013.04.009

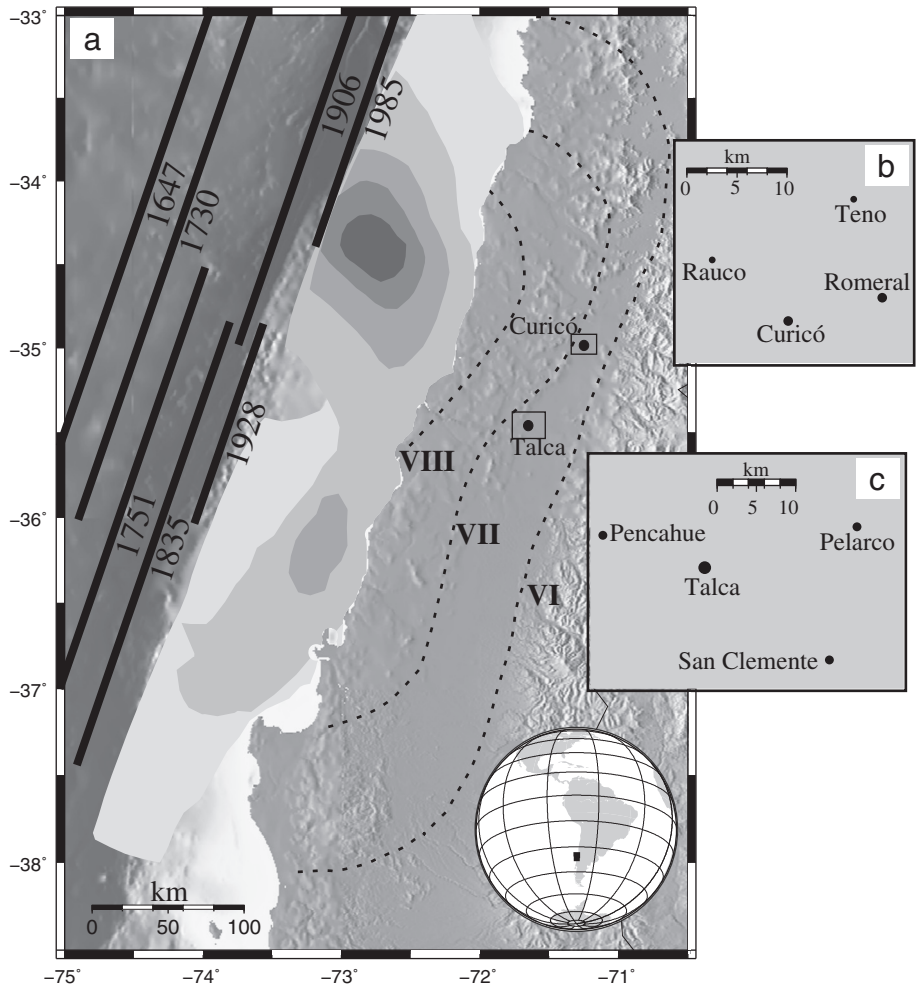

Fig. 1. (a) Digital elevation model with the location of Talca and Curicó, Central Chile, the insert show the location of the studied area. The dashed lines show the isoseismals for hard soil conditions for the 2010 Maule earthquake, with the level in roman numbers (Astroza et al., 2012); while in shades of gray is presented the slip distribution of this event, obtained by Lay et al. (2010). Thick lines show schematically the rupture length of large earthquakes, with its corresponding year of occurrence next to each one. (b) and (c) shows a detail map of nearby cities of Curicó and Talca, respectively.

localities, reported seismic intensities are consistently lower: Pencahue (IMSK64 = VI–VII) and San Clemente (IMSK64 = VI–VII).

Recently, for the 2010 Maule earthquake (Mw 8.8), Curicó presented an IMSK64 = VII–VIII, while nearby cities showed lower intensities: Teno (IMSK64 = VII), Rauco (IMSK = VII), and Romeral (IMSK64 = VI). Talca presented an IMSK64 = VIII, whereas nearby cities showed clearly lower intensities: Pelarco (IMSK64 = VI–VII), Pencahue (IMSK64 = VII), and San Clemente (IMSK64 = VI–VII). Even more, considering that both cities are located near the isoseismal VII (see Figure 1 and caption for details), the seismic intensities observed in Talca and Curicó represent an increment of 1.0 and 0.5°, respectively, with respect to hard soil conditions (Astroza et al., 2012). These amplifications cannot be explained by the distance from the source, but presumably by local effect conditions. To further explore this hypothesis, we performed a high-density macroseismic study considering the distribution of the damage within each city: nearly 700 field surveys were carried out few days after the earthquake, assigning IMSK64 to all the urban areas. The observed distribution of MSK intensities was very irregular, which we believe was strongly influenced by local site amplification, more than by epicentral distance, location of asperities within the fault and/or path effects.

To assess the local site conditions, we revised the surface geology at both localities using all available data. We found a strong presence of alluvial and fluvial deposits (in Curicó and Talca) along with volcanic ash deposits (in Talca). We complement this information by performing nearly 300 microtremor measurements at Talca and Curicó, covering the entire studied area. Several studies have shown a correlation between the peak observed in microtremors' HVSR and site amplification (Lermo and Chávez-García, 1993; Bard, 1999; Bonnefoy-Claudet et al., 2006; Chávez-García et al., 2007); however, only in few cases these results had been compared with direct observation of damage produced by a large earthquake. We found a strong correlation between microtremors' HVSR and surface geology: the comparison at Talca is quite clear; while at Curicó there are other factors to take into account. This correlation is the best way to explain the observed distribution of damage at Curicó and Talca; hence, we believe that the combination of surface geology and microtremors' HVSR represents a practical and economical method to assess local site conditions and possible seismic amplifications.

2. Geological setting

The cities of Talca and Curicó are located in the Central Depression, a North–south trending morphostructural unit of lowlands between the Coastal and Main ranges of the Andes (Figure 1). The Central Depression is filled with alluvial sediments transported from the highlands and some volcanic ash deposits from large Quaternary eruptions, forming the sedimentary basins where Talca and Curicó are located. The Coastal Range, located to the West of the depression, is mainly composed of intrusive and volcanosedimentary rocks of Paleozoic and Mesozoic age while the Main Range, located to the East, is formed by Tertiary volcanic and intrusive rocks and Quaternary volcanic rocks and deposits from

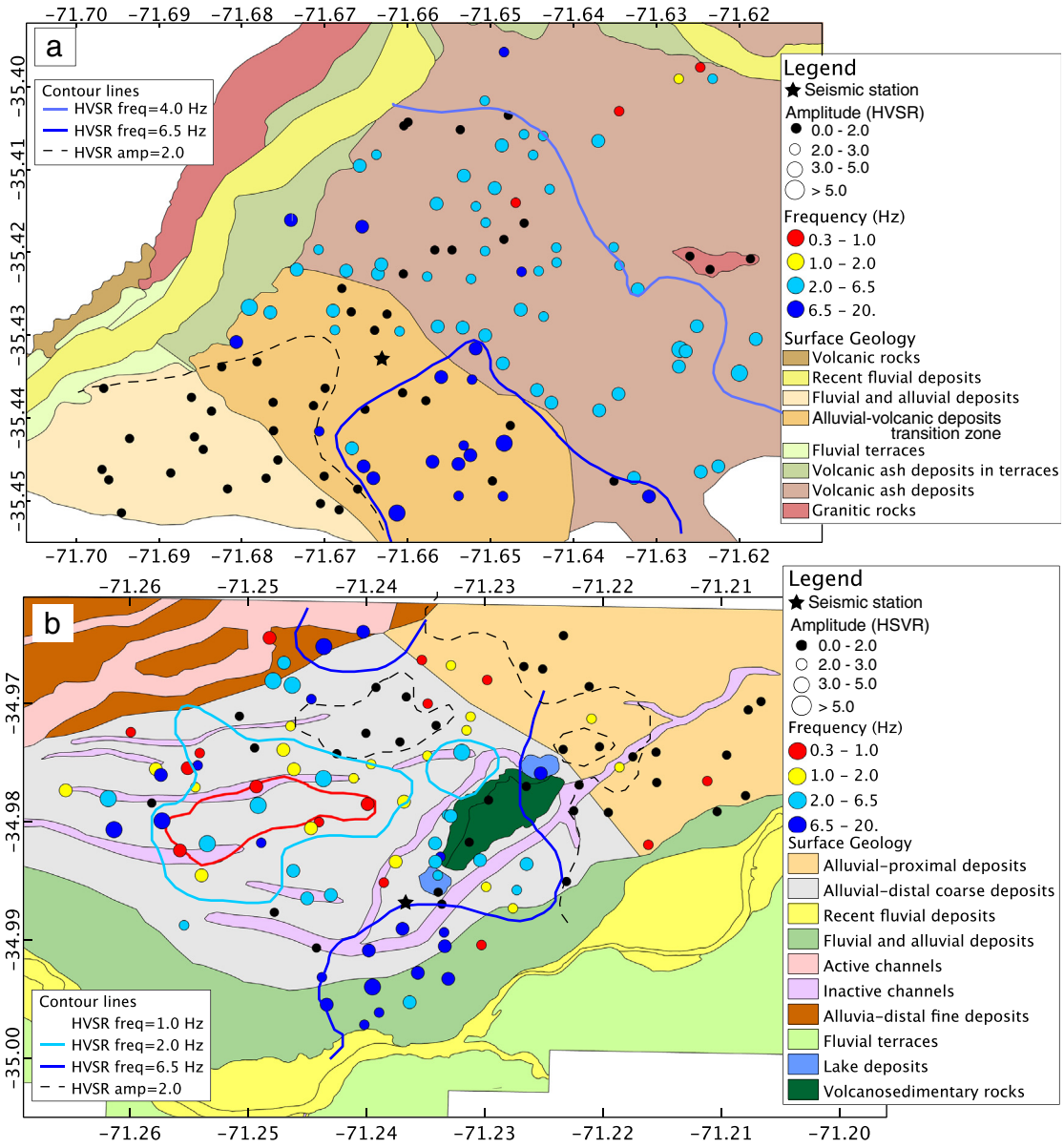

Fig. 2. Surface geology of: (a) Talca and (b) Curicó, see corresponding legends on the right. The circles represent microtremors' HVSR, with the color proportional to the estimated resonance frequency and the size to its amplitude, following the scale on the right. The black stars mark the position of the seismic stations that recorded the Maule 2010 earthquake. We also plotted some contour lines of resonance frequency and HVSR amplitude, indicated in the insets on the right.

the present volcanic arc (Hauser, 1995; Sernageomin, 2003). The local geology of Talca and Curicó has been previously described by Hauser (1995) and in unpublished maps by Thiele (in Morales and Sapaj, 1996); in the present study, we report a detailed revision of the surface geology of these localities.

The distribution of the deposits of Talca has been revised by inspection of about 30 logs of 35–50 m deep boreholes drilled by the local water company; the modified geological map of Talca is shown in Fig. 2(a). We find three main units that practically cover all the urban area: i) to the Southwestern part of the city, fluvial deposits of gravel and sand with clay interbeds that are part of the alluvial fan of the large Maule river, located about 15 km south of the city, ii) to the Northern part of the city, volcanic deposits of ash, lapilli, and pumice, and iii) a transition zone between the former deposits, in which the alluvial and volcanic deposits are interbedded in a complex manner. The volcanic deposits present flow textures, and have been suggested to be originated by a large Pleistocene pyroclastic flow from the Descabezado or Calabozos volcanic group, located about 80 km to the ENE, that reached the central depression through the Claro River valley (Hildreth et al., 1984; Hauser, 1995; Morales and Sapaj, 1996). Talca is surrounded by the Lircay River (to the North) and the Claro River (to the West), with terraces of alluvial and volcanic sediments on their margins, along with present fluvial deposits (Figure 2(a)). The western part of the city is limited by the foothills of the Coastal Range, with outcrops of volcanic and intrusive rocks partly covered by talus, while the eastern part is covered by volcanic deposits with exception of local hills, of granitic composition (Figure 2(a)). The water table varies between about 5 and 20 m of depth, depending on location and climatic fluctuations (Hauser, 1995).

The local geology of the urban area of Curicó was revised by detailed surface mapping (Figure 2(b)). The city is mainly built on alluvial deposits from the Teno River, mostly characterized by gravel deposits in a sand and silt matrix, with a prevalence of coarse-grained materials in the proximal deposits to the East, and a progressively increasing presence of fine-grained material in the distal deposits, to the West. These deposits are cut by several fluvial inactive channels and lacustrine

deposits, which concentrate sand and fine-grained soil banks. Towards the South, the alluvial deposits vary to fluvial terraces and the active fluvial channels of Huaiquillo creek and Mataquito River. An isolated hill composed of Cretaceous volcanosedimentary rocks, known as Condell hill, outcrops in the middle of the city. The water table is located in general less than 5 m deep, which makes the sandy and fine grained deposits prone to liquefaction, as locally observed during the 2010 earthquake North and Northwest of Condell hill.

3. Microtremors' HVSR

We performed an extensive campaign of more than 170 and 110 microtremors' measurements at Talca and Curicó, respectively, using a 3-component, 4.5-Hz instrument; Strollo et al. (2008a,b) showed that short-period sensors are able to retrieve resonance frequencies up to 0.1 Hz, furthermore, Leyton et al. (2011) showed that these instruments are able to obtain a reliable answer from 0.3 up to 20 Hz. At each point, we recorded microtremors for at least 20 min, depending on the level of human activity, as recommended for microzonation studies (Bard and SESAME-Team, 2005). Later, each measurement was processed in the same way: firstly, we divided the total time window into 1 min subwindows, not removing the transients, following Parolai and Galiana-Merino (2006). Then, we computed the Fourier transform and smoothed it with a homogenous filter in log-scale (Konno and Ohmachi, 1998), and calculate the horizontal-to-vertical spectral ratio (HVSR). Due to the fact that we used 1 min subwindows, we obtain at least 20 subwindows without overlap, and calculated the measurement precision for each frequency by means of the standard deviation.

After processing all the measurements, the resulting HVSR curves were classified into 4 groups, as shown in Fig. 3, having the following classification:

(a) A clear peak, with large amplitude (over 5.0)
(b) A clear peak, with medium amplitude (between 3.0 and 5.0)
(c) A diffuse peak, with low amplitude (between 2.0 and 3.0)
(d) Flat curve, with no clear peak (amplitudes lower than 2.0).

Previous studies showed that the presence of large amplitude HVSR peak is related to a high impedance contrast between the sedimentary cover and the basement (Bard, 1999; Bonnefoy-Claudet et al., 2006, 2008b), while a low amplitude peak is related to a lower contrast, indicating the presence of a hard soil (Woolery and Street, 2002; Bonnefoy-Claudet et al., 2006, 2008b). In the present study, cases (a), (b), and (c) of Fig. 3 enable a reliable estimation of the fundamental frequency from the observed HVSR peaks, probably related to the presence of soft soil with a high impedance contrast with the basement. On the other hand, in the presence of hard soils, it is not possible to find a clear contrast that generates a resonance frequency at the site, thus a flat HVSR curve is observed in such a situation (Bonnefoy-Claudet et al., 2008a; Leyton et al., 2011), as shown in case (d) of Fig. 3. This same behavior is observed at rock sites, as can be seen as black dots at the outcrops of Talca (granitic rocks) and Curicó (volcanosedimentary rocks) in Fig. 2. Due to the lack of detailed geophysical information, we cannot further describe the characteristics of the basement rock or shape of the sedimentary basins. On the other hand, as shown in Fig. 2, accelerometers were placed on both cities and successfully recorded Maule 2010 earthquake (Boroschek et al., 2010); in the Supplementary Figure, we present a

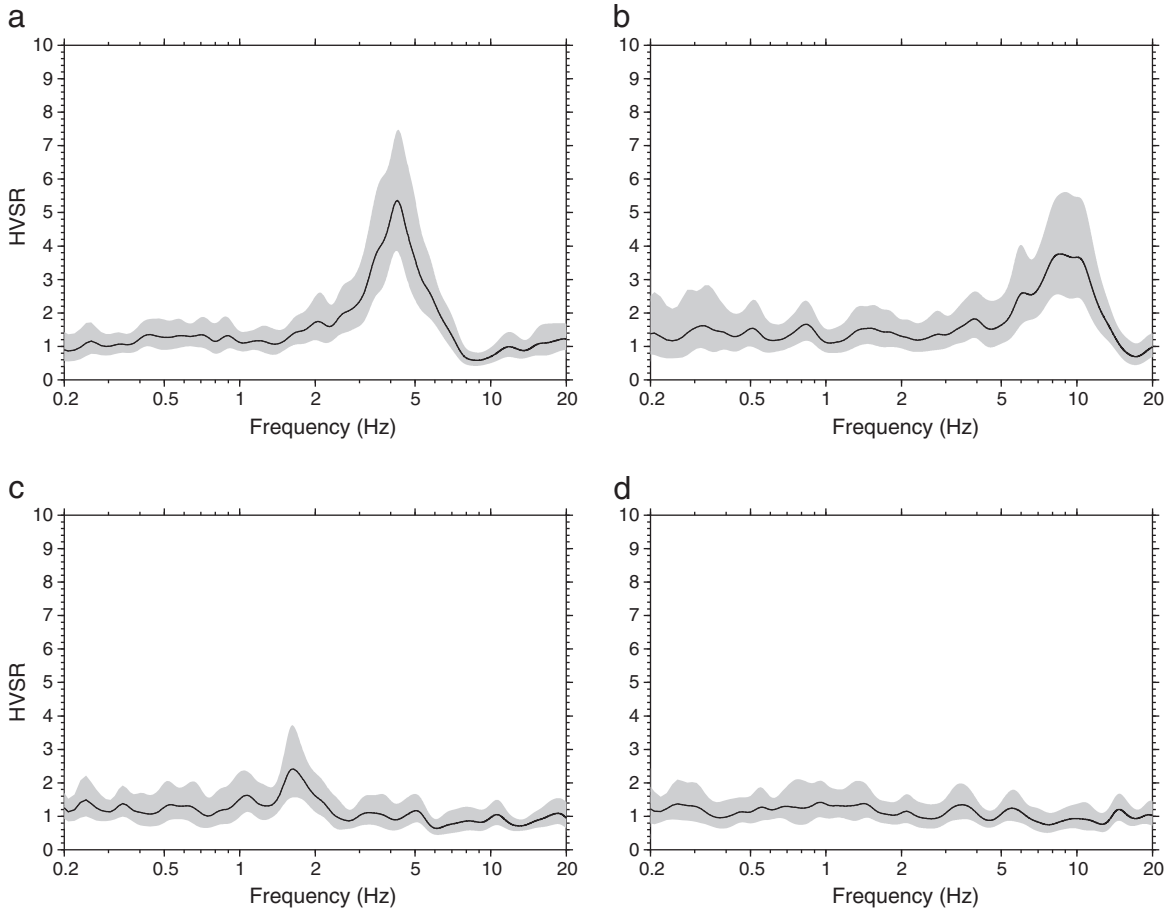

Fig. 3. Classification of the microtremors' HVSR from Talca and Curicó; continuous line shows the geometric average, while the gray area corresponds to the standard deviation. See text for details.

comparison of the HVSR between the strongmotion records and the microtremors.

Despite the scatter in the results, Fig. 2 shows a strong correlation between surface geology and the soils' resonance frequency. This correlation is enhanced with the contour lines for HVSR's estimated frequencies and amplitudes plotted in Fig. 2. At Talca (Figure 2a), we can see that the volcanic ash deposits are characterized by resonance frequencies ranging from 2.0 to 6.5 Hz (cyan circles in Figure 2(a)), mostly from 4.0 to 6.5 Hz as shown by the contour lines, with amplitudes going from small (between 2.0 and 3.0) to large (>5.0). On the other hand, the fluvial and alluvial deposits are mostly characterized by flat HVSR curves (black dots in Figure 2(a)) or small amplitude peaks (lower than 3.0). Finally, the alluvial-volcanic transition zone presents high resonance frequencies (larger than 6.5 Hz, shown in blue in Figure 2a) in its Southeastern part, turning into flat curves to the northwest (black dots). In this region we found some sites with resonance frequencies between 2.0 and 6.5 Hz, mostly to the Northeastern part, showing the transition to the volcanic ash deposits.

At Curicó (Figure 2b), we found a more complicated setting: the Northeastern part, in the alluvial-proximal deposits, was mainly characterized by flat HVSR curves (black dots in Figure 2b) or small amplitude peaks (lower than 3.0), correlating with the presence of coarse-grained materials. Towards the West, we found the alluvial–distal finer deposits, characterized by low frequencies (lower than 1.0 Hz, shown in red in Figure 2b) and large amplitudes (usually, greater than 3.0). In the alluvial–distal coarse deposits, mostly throughout the city of Curicó, we found clear resonance frequencies, ranging from 0.3 to 6.5 Hz (red, yellow, and cyan circles in Figure 2b), with a variety of amplitudes. As mentioned before, throughout the city of Curicó it is observed the presence of fluvial inactive channels and lacustrine deposits, the most probable mechanism of fine-grained material deposition in the area, producing the low frequencies observed (red and yellow circles in Figure 2b); however, the microtremors' HVSR is not sensitive enough to clearly identify them, probably due to their small thickness. In the Southern part of the city, at the transition to fluvial and alluvial deposits, we found high resonance frequencies and large amplitude peaks (shown in cyan for frequencies between 2.0 and 6.5 Hz and in blue for frequencies higher than 6.5 Hz in Figure 2b), marking the relationship between high frequencies and the presence of coarse-grained materials.

4. Damage observed after the 2010 Maule Earthquake

The damage distribution observed at Talca and Curicó after the 2010 Maule earthquake was non homogenous, justifying the first high-density macroseismic survey at these cities. We followed Monge and Astroza (1989) to estimate the seismic intensity variations within the city; this methodology has been successfully applied to an extensive survey of more than 100 localities affected by the Maule 2010 earthquake (Astroza et al., 2012).

We performed nearly 700 field surveys in both localities, which cover the entire study area (~300 at Curicó and ~400 at Talca), and assigned MSK64 intensity to each sector, completing 19 and 11 sectors at Talca and Curicó, respectively (see Figure 4a and b). The definition of the sectors at each city considered surface geology and the distribution of vulnerability classes in the area: using 1-km^2 sectors, we tried to include low-rise buildings belonging to one vulnerability class within each sector (labels shown in Figure 4). Finally, we defined each sector's intensity from the observed damage, taking into account the structural vulnerability class of the constructions (Monge and Astroza, 1989), as shown in Fig. 5. This figure shows the mean damage grade (Gm, computed as a weighted average of the number of construction within a vulnerability class, weighted by the observed level of damage, see Monge and Astroza, 1989) as a function of the corresponding MSK seismic intensity and the vulnerability class (shown in dashed lines in Figure 5). From this figure we can see that 2 sectors with the different vulnerability class present very different mean damage grade; the complete data is shown in the supplementary material (Table S1).

Fig. 4a and b shows the defined sector and its corresponding results, each symbol represents a vulnerability class (ranging from A, most vulnerable, to C, least vulnerable), the colors represent the level of damage (ranging from 0, no damage, to 5, collapse of one or more walls), and the pattern the MSK seismic intensity.

The highest intensity we found was in volcanic ash deposits at Talca, reaching VIII degree on the MSK64 scale (shown in Figure 4a). In this area, most of the adobe houses (vulnerability class A) suffered heavy damage or collapse, whereas reinforced masonry house (vulnerability class C) presented a range of cracks from small to severe. The intensity in different sectors of both cities ranged from VI up to VIII on the MSK64 scale; we believe that the main responsible of these variations are the surface geological conditions, also reflected in the variations of the resonance frequencies of the soils. At Talca, considering only the sectors over the volcanic ash deposits, we found lower intensities at places located at the Northeastern side of the city (sectors 6 and 13); this could be produced by an underestimation of the vulnerability class of the housing found in this area. From field observations, class D, rather than class C as used in this study, might be a better characterization for most of the houses because they are engineered masonry buildings with earthquake-resistant design (Grünthal, 1998).

5. Discussion and conclusions

As presented in Figs. 2 and 6, as discussed below, we found a strong correlation between surface geology and the soils' predominant frequency. In general, fine-grained soils are characterized by frequencies ranging from 0.3 up to 6.5 Hz. On the other hand, coarse-grained materials are characterized by high frequencies (higher than 6.5 Hz) and flat HVSR curves. Talca presented, at volcanic ash deposits, resonance frequencies between 2.0 and 6.5 Hz, while fluvial and alluvial deposits were characterized by flat HVSR curves. Even at Curicó, where there is a complex distribution of the resonance frequencies, it can be explained with recent findings of disaggregation of an alluvial fan, mainly related with old superficial channels. In the Northwestern part of the city, over the alluvial-proximal deposits, we found low amplitude peaks (lower than 3.0) and flat HVSR curves. On the other hand, the alluvial–distal coarse deposits, found throughout the city of Curicó, are characterized by large amplitude peaks (greater than 3.0) with resonance frequencies lower than 6.5 Hz (see Figure 6b). All these areas are cut by several inactive channels, probably the cause of deposition of fine-grained materials, producing the observed low resonance frequencies.

From the high-density macroseismic observations, we found MSK64 intensities ranging from VI up to VIII, strongly dominated by surface geology, as it can be seen in Fig. 6. Even more, from this figure we found a strong correlation between the observed intensities (overlaying patterns) and resonance frequencies (colored pie charts) observed at these two localities. Indeed, lower intensities are found in areas characterized by flat HVSR curves and the presence of coarse-grained materials. On the other hand, the higher intensities are observed at sites characterized by clear peaks, with frequencies ranging from 0.3 to 6.5 Hz, at Curicó, and 2.0 to 6.5 Hz, at Talca.

In summary, we found a strong variation of the damage produced by a large earthquake (Mw 8.8), mainly explained by surface geology and observed resonance frequencies (from microtremors' HVSR). This correlation can be used in the definition of different seismic zones within each city, indicating an inexpensive and effective methodology for seismic microzonation studies.

Supplementary data to this article can be found online at http://dx.doi.org/10.1016/j.enggeo.2013.04.009.

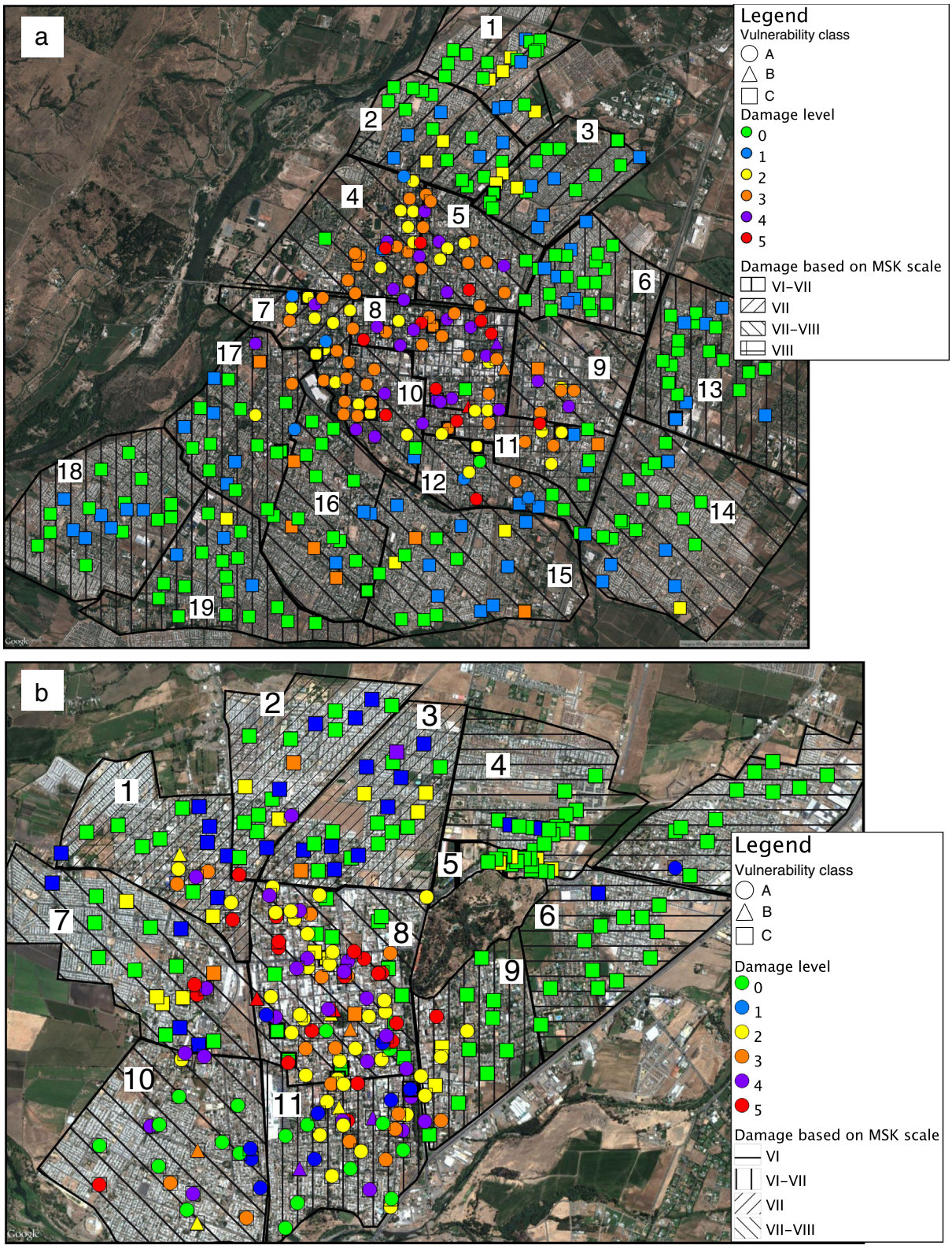

Fig. 4. Aerial photograph of: (a) Talca and (b) Curicó, showing the distribution of surveys made to estimate the macroseismic intensities at each sectors; these are marked with black lines and labeled with numbers. Each symbol represents a vulnerability class while the colors show the damage level; the overlaying patterns show the distribution of MSK64 intensity at each sector, see scale on the left.

Acknowledgments

The authors would like to thank the invaluable help of J. Maripangui and V. Soto during the fieldwork and the National Seismological Service for facilitating the instruments used in this study. We would like to acknowledge the Dept. Civil Engineering of the Universidad de Chile for making the data of the Maule 2010 freely available to the scientific community. This work was financed by Fondecyt 1100551 and Millennium Nucleus of Seismotectonics and Seismic Hazard. We would like to thank M. Lara for her assistance preparing the maps; figures used QGIS

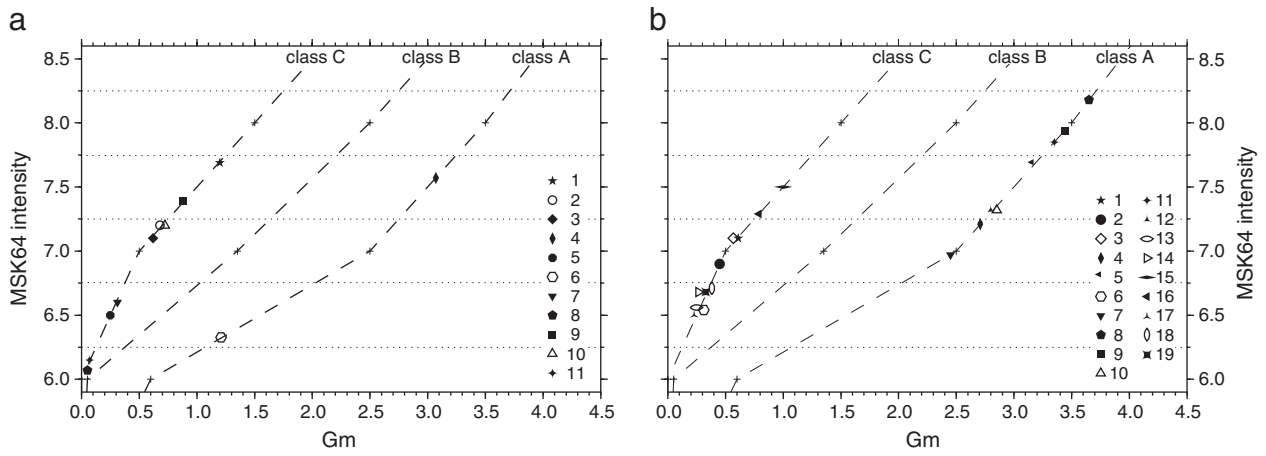

Fig. 5. MSK64 seismic intensity as a function of the mean damage level (Gm) and the vulnerability class (dashed lines) for (a) Talca and (b) Curicó; see text for details. Each symbol represents a sector, following the legend on the right.

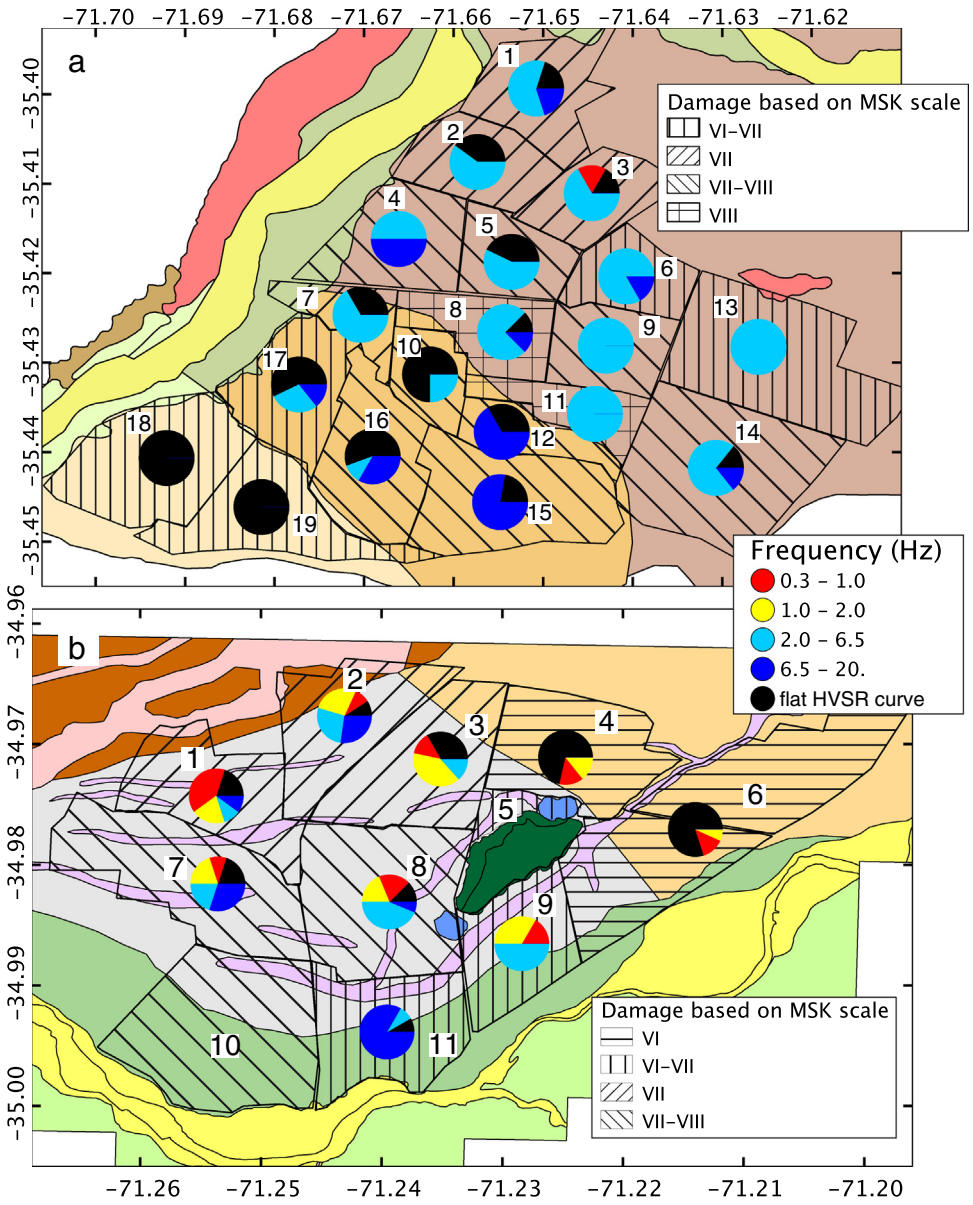

Fig. 6. Summary of predominant frequencies observed in each sector at: (a) Talca and (b) Curicó. The pie charts show the percentage of resonance frequencies observed in each sector, following the color code shown in the middle, while the patterns indicate the MSK64 intensity for the Maule 2010 earthquake. The colors represent the surface geology; see legends at Fig. 2(a) and (b).

and GMT (Wessel and Smith, 1991). We would also like to thank 2 anonymous reviewers for their comments that greatly improving the manuscript.

References

Astroza, M., Moya, A., Sanhueza, Y., 2002. Estudio comparativo de los efectos de los terremotos de Chillán de 1939 y de Talca de 1928. VIII Jornadas Chilenas de Sismología e Ingeniería Antisísmica, Valparaiso, Chile (In Spanish).

Astroza, M., Ruiz, S., Astroza, R., 2012. Damage assessment and seismic intensity analysis of the 2010 (Mw 8.8) Maule earthquake. Earthquake Spectra 28 (81), S145–S164.

Bard, P.Y., 1999. Microtremors measurements: a tool for site effect estimation? The Effects of Surface Geology on Seismic Motion, vol 3. Balkema, Rotterdam, pp. 1251–1279.

Bard, P.Y., SESAME-Team, 2005. Guidelines for the implementation for the H/V spectral ratio technique on ambient vibrations-measurements, processing and interpretations. SESAME European Research Project EVG1-CT-2000-00026, Deliverable D23.12 (available at http://sesame-fp5.obs.ujf-grenoble.fr.).

Barrientos, P., Cancino, J.M., 1991. Estudio de los efectos del sismo del 3 de marzo de 1985 en la Séptima Región, Dissertation for Civil Engineering Degree. Universidad de Chile, Santiago, Chile (In Spanish).

Bonnefoy-Claudet, S., Cornou, C., Bard, P.Y., Cotton, F., Moczo, P., Kristek, J., Fäh, D., 2006. H/V ratio: a tool for site effects evaluation. Results from 1-D noise simulations. Geophysical Journal International 167, 827–837.

Bonnefoy-Claudet, S., Baize, S., Bonilla, L.F., Berge-Thierry, C., Pasten, C., Campos, J., Volant, P., Verdugo, R., 2008a. Site effect evaluation in the basin of Santiago de Chile using ambient noise measurements. Geophysical Journal International 176 (3), 925–937.

Bonnefoy-Claudet, S., Köhler, A., Cornou, C., Wathelet, M., Bard, P.Y., 2008b. Effects of Love waves on microtremor H/V ratio. Bulletin of the Seismological Society of America 98 (1), 288–300.

Borcherdt, R.D., 1970. Effects of local geology on ground motion near San Francisco Bay. Bulletin of the Seismological Society of America 60, 29–61.

Boroschek, R., Soto, P., Leon, R., Comte, D., 2010. Registros del Terremoto del Maule 2010 Mw = 8.8, 27 de Febrero de 2010. Informe del Depto de Ingeniería Civil — Depto de Geofísica.Universidad de Chile (In Spanish).

Chávez-García, F.J., Dominguez, T., Rodriguez, M., Pérez, F., 2007. Site effects in a volcanic environment: a comparison between HVSR and array techniques at Colima, Mexico. Bulletin of the Seismological Society of America 97, 591–604.

European macroseismic scale 1998. In: Grünthal, G. (Ed.), Cahiers du Centre Européen de Géodynamique et de Séismologie, Vol. 15, pp. 1–99 (Luxembourg).

Hauser, A., 1995. Carta Hidrogeológica de Chile. Hoja Talca, VII Región, Escala 1:100.000. 73 p. (In Spanish).

Hildreth, W., Grunder, A.L., Drake, R.E., 1984. The Loma Seca Tuff and the Calabozos Caldera: a major ash-flow and caldera complex in the southern Andes of central Chile. Geological Society of America Bulletin 97, 45–54.

Holzer, T.L., 1994. Loma Prieta damage largely attributed to enhanced ground shaking. EOS. Transactions of the American Geophysical Union 75, 299–301.

Konno, K., Ohmachi, T., 1998. Ground-motion characteristics estimated from spectral ratio between horizontal and vertical components of microtremor. Bulletin of the Seismological Society of America 88 (1), 228–241.

Lay, T., Ammon, C.J., Kanamori, H., Koper, K.D., Sufri, O., Hutko, A.R., 2010. Teleseismic inversion for the rupture proces if the 27 Febreart 2010 Chile (Mw 8.8) earthquake. Gephys. Res. Lett. 37. http://dx.doi.org/10.1029/2010GL043370.

Lermo, J., Chávez-García, F.J., 1993. Site effect evaluation using spectral ratios with only one station. Bulletin of the Seismological Society of America 83, 1574–1594.

Leyton, F., Sepulveda, S.A., Astroza, M., Rebolledo, S., Acevedo, P., Ruiz, S., Gonzalez, L., Foncea, C., 2011. Seismic zonation of the Santiago Basin, Chile. 5th International Conference on Earthquake Geotechnical Engineering, Santiago, Chile.

Milne, J., 1898. Seismology. Kegan Paul, Trench, Truber, London.

Monge, J., Astroza, M., 1989. Metodología para determinar el grado de intensidad a partir de los daños, 5as. Jornadas Chilenas de Sismología e Ingeniería Antisísmica, Vol. Nº1, pp. 483–492 (Santiago, Chile. (In Spanish)).

Montessus de Ballore, F., 1915. Historia Sísmica de los Andes Meridionales al Sur del Paralelo XVI, Quinta Parte. El Terremoto del 16 de Agosto de 1906.Soc. Imprenta-Litografía Barcelona, Santiago, Chile (In Spabish).

Morales, D., Sapaj, R., 1996. Riesgo sísmico de las ciudades de Curicó, Molina, Talca, San Clemente, Constitución, Linares, San Javier, Parral y Cauquenes. Dissertation for Civil Engineering Degree. Universidad de Chile, Santiago, Chile (In Spanish).

Ordaz, M., Singh, S.K., 1992. Source spectra and spectral attenuation of seismic waves from Mexican earthquakes, and evidence of amplification in the hill zone of Mexico City. Bulletin of the Seismological Society of America 82, 24–43.

Parolai, S., Galiana-Merino, J.J., 2006. Effect of transient seismic noise on estimates of H/V spectral ratios. Bulletin of the Seismological Society of America 96 (1), 228–236. http://dx.doi.org/10.1785/0120050084.

Sernageomin, 2003. Mapa Geológico de Chile: Versión Digital. Servicio Nacional de Geología y Minería, Publicación Geológica Digital Nº4. (In Spanish).

Singh, S.K., Lermo, J., Dominguez, T., Ordaz, M., Espinosa, J.M., Mena, E., Quass, R., 1988. The Mexico earthquake of September 19, 1985 — a study of amplification of seismic waves in the valley of Mexico with respect to a hill zone site. Earthquake Spectra 4, 653–673.

Strollo, A., Parolai, S., Jäckel, K.H., Marzorati, S., Bindi, D., 2008a. Suitability of short-period sensors for retrieving reliable H/V peaks for frequencies less than 1 Hz. Bulletin of the Seismological Society of America 98 (2), 671–681.

Strollo, A., Bindi, D., Parolai, S., Jäckel, K.H., 2008b. On the suitability of 1 s geophone for ambient noise measurements in the 0.1–20 Hz frequency range: experimental outcomes. Bulletin of Earthquake Engineering 6 (1), 141–147.

Wald, L.A., Mori, J., 2000. Evaluation of methods for estimating linear site-response amplifications in the Los Angeles region. Bulletin of the Seismological Society of America 90, S32–S42.

Wessel, P., Smith, W.H.F., 1991. Free software helps map and display data. EOS. Transactions of the American Geophysical Union 72, 441.

Woolery, E.W., Street, R., 2002. 3D near-surface soil response from H/V ambient-noise ratios. Soil Dynamics and Earthquake Engineering 22, 865–876.